



Title	Selection and transfer of individual plasmon-resonant metal nanoparticles
Author(s)	Tanaka, Yoshito; Sasaki, Keiji
Citation	Applied Physics Letters, 96(5), 053117 https://doi.org/10.1063/1.3304085
Issue Date	2010-02-01
Doc URL	https://hdl.handle.net/2115/42640
Rights	Copyright 2010 American Institute of Physics. This article may be downloaded for personal use only. Any other use requires prior permission of the author and the American Institute of Physics. The following article appeared in Appl. Phys. Lett. 96, 053117 (2010) and may be found at https://dx.doi.org/10.1063/1.3304085
Type	journal article
File Information	APL96-5_053117.pdf



Selection and transfer of individual plasmon-resonant metal nanoparticles

Yoshito Tanaka and Keiji Sasaki^{a)}

Research Institute for Electronic Science, Hokkaido University, Sapporo 001-0020, Japan

(Received 16 November 2009; accepted 12 January 2010; published online 5 February 2010)

We present a simple method for selecting a single metal nanoparticle with desired localized surface plasmon (LSP) characteristics from particle ensembles on one surface and then transferring it to another surface. The LSP of individual nanoparticles is characterized using a microspectroscopy system. An atomic force microscope mounted on the optical microscope achieves particle capture and release with the chemically modified probe. © 2010 American Institute of Physics. [doi:10.1063/1.3304085]

Gold and silver nanoparticles typically exhibit strong optical resonance in the visible wavelength range due to collective oscillations of conduction electrons in the nanoparticles known as localized surface plasmon (LSP),¹ which has long fascinated scientists. The LSP not only gives the nanoparticle a specific color but also enables concentration of electromagnetic fields on the nanoscale, while enhancing local field strengths by several orders of magnitude. These give rise to a range of physically interesting and technologically important phenomena. These phenomena include surface enhanced Raman scattering (SERS),²⁻⁴ fluorescence enhancement,⁵ nanoscale lithography,^{6,7} and nonlinear photochemical reactions.⁸ The LSP characteristics sensitively depend on particle size, shape, and dielectric environment.¹ For applications in nano-optics, there is a clear requirement for metal nanoparticles with optimized LSP characteristics. For example, the frequency of LSP resonance should match with the excitation wavelength, and the dephasing time $T=2\hbar/\Gamma_{\text{hom}}$, where Γ_{hom} is the homogeneous linewidth of the LSP resonance, of LSP excitation should be as large as possible.^{9,10} In fact, the demand for optimized LSP performance is more critical in applications of single-molecule SERS.^{11,12} Consequently, much effort has recently been dedicated to the control of LSP characteristics. For this purpose, a large variety of particle sizes and shapes were obtained using chemical synthesis and electron beam lithography. However, the chemical fabrication approaches do not allow a perfect control of the particle geometry. On the other hand, the electron lithography method can produce nanoparticles having precise sizes and shapes on the substrate but it is not adaptable for substrate compositions that are easily changed or degraded in wet environments because this method includes a wet process.

Here, we report a combination technique of atomic force microscopy (AFM) and single-particle spectroscopy that allows us to select individual nanoparticles with desired LSP characteristics from particle ensembles spread on one surface and then transfer it to another surface in an air environment. Figure 1 schematically illustrates the setup. The LSP of nanoparticles is characterized by their Rayleigh scattering spectra. An unpolarized white light from a halogen lamp was introduced into an inverted microscope (Olympus, IX-71) and a sample was illuminated via an oil immersion objective lens (Olympus UPlanApo 100×, N.A.=1.35). For dark-field

illumination, a knife edge was placed at the pupil plane of the imaging system and used to mask a part of the white light. Thus, when the knife edge is removed, bright-field illumination was available. In both cases, the illumination area was approximately 30 μm in diameter. The Rayleigh-scattered light was collected by the same microscope objective, passed through an optical fiber, and directed to a multichannel photodetector (Hamamatsu Photonics, PMA-11). The collection area was nearly 2.5 μm in diameter for the objective/fiber combination used here. The scattering spectra were corrected for the intensity distribution of the incident white light. To prepare the sample, we spin coated colloidal gold nanoparticles of 100 nm mean diameter (British Biocell International) onto a microscope cover glass with a dilute coverage of the order of one particle per $3 \times 3 \mu\text{m}^2$, as shown in Fig. 2(a). Each spectrum of the bright spots observed in Fig. 2(a) was measured separately. For particle manipulation, a commercial AFM head (Veeco, diCaliber) was situated on top of the optical microscope. The position of the AFM tip was determined under bright-field observation. The scan range was set at the collection area of the scattered light. Tapping mode AFM was conducted in its region to attach a target particle with well-defined optical properties to the end of the probe.

For glue between the tip and gold nanoparticle, the surface properties of the probes are modified by treatment with a silane coupling agent having an amino group. A silicon

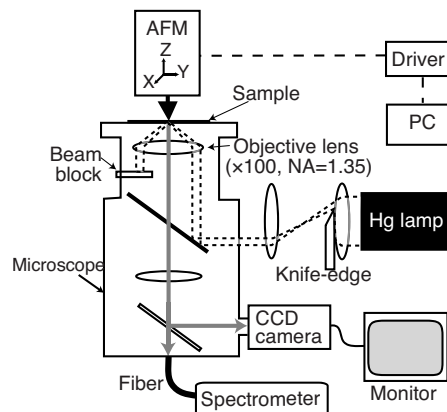


FIG. 1. Schematic diagram of the experimental setup of combined AFM and single-particle spectroscopy. White light from an Hg lamp illuminates gold nanoparticles under dark-field condition. The scattered light from a single particle is collected and sent to a spectrometer. AFM on the optical microscope is used to capture and release individual particles.

^{a)}Author to whom correspondence should be addressed. Electronic mail: sasaki@es.hokudai.ac.jp.

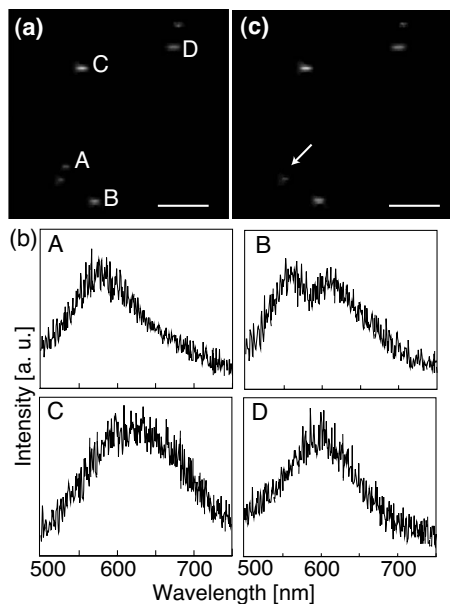


FIG. 2. (a) Dark field image and (b) spectra of gold nanoparticles spread on a glass substrate. The symbols on the image indicate places where the spectra were taken. An AFM tip coated with amino groups approached the particle indicated by symbol “A.” After establishing contact with the target, its tip captures the particle. (c) Dark-field image of the same area as in (a) after this procedure, confirming that the chosen particle has left the substrate. Its former position is indicated by an arrow. The illumination area is $\sim 30 \mu\text{m}$ in diameter. Bar = $5 \mu\text{m}$.

AFM probe (Olympus OMCL-AC160TS-C2) was initially cleaned by UV/ozone for 20 min to facilitate the silanization. We use a gas-phase method based on Ref. 13 to modify the surface of the probe with 3-aminopropyltrimethoxysilane (APTMS; Tokyo Kasei Kogyo) molecules. Gas-phase preparations have been proven to produce better quality surfaces than liquid preparation.^{13,14} In short, a nitrogen flow of approximately 1 L/min was used to increase the evaporation rate of the silane molecules by lowering the partial pressure of the silane molecules in the gas phase above the liquid silane, at room temperature and atmospheric pressure. Thus, an increased number of molecules came into contact with the silicon oxide surface of the probe placed in the reactor. It should be noted that all treatments were performed under dry condition, which is effective for surface chemical modification of fragile objects like AFM probes and also for material compositions that are easily changed or degraded in wet environments.

The captured nanoparticle is then released onto another surface. This is based on a higher affinity of thiol groups for the surface of the metal nanoparticles than amino groups. Thus, a cover-glass surface was coated with a monolayer of 3-mercaptopropyltrimethoxysilane (MPTMS; Tokyo Kasei Kogyo), according to the same gas-phase procedure as that used for APTMS. This coverslip was exchanged with one used in the particle-capture process. The particle attached on the end of the tip was then placed in contact with the coverslip using a force-control system of AFM.

LSP characteristics of gold nanoparticles on glass were clearly different from each other as shown in Fig. 2. This can be mainly attributed to the diversity of particle sizes and shapes. The past experimental and theoretical studies indicated that the spectral change due to interparticle coupling on the particle plasmon resonances becomes negligible when

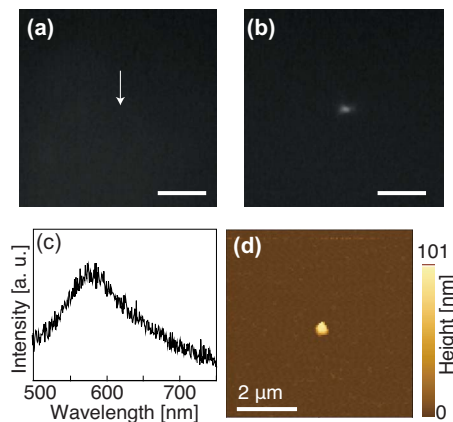


FIG. 3. (Color online) Dark-field images of a glass substrate coated with thiol groups (a) before and (b) after touching the particle attached on the tip to the surface. The arrow in (a) indicates the position where the captured particle was placed in contact with the surface. The illumination area is $\sim 30 \mu\text{m}$ in diameter. Bar = $5 \mu\text{m}$. (c) Spectrum and (d) AFM image of a gold nanoparticle released from an AFM tip.

the center-to-center distance between neighboring nanoparticles exceeds about twice the particle size.^{1,15} Thus, although the particle indicated by symbol “A” has the nearby particle, its spectrum corresponds to that of the isolated particles because of their interparticle distance more than $1 \mu\text{m}$. On the other hand, the particle indicated by symbol “B” can be considered as multiple particles with significant plasmon coupling or an anisotropic particle like a rod and a triangular prism from the spectral shape of Fig. 2(b)-B.^{1,16} Here, we select the particle “A” as a target particle. When a tapping AFM tip establishes contact with the target particle, it lifts the particle, resulting in the absence of the bright spot in the dark-field image [Fig. 2(c)]. In the release step shown in Fig. 3, no light scattering objects were observed on another prepared surface. The particle release is performed under microscope observation. The bright spot appeared just after the captured particle touched the surface. The spectrum of this released particle was in fair agreement with one of the target particles. Furthermore, it was confirmed to be a single gold nanoparticle of 100 nm in diameter by its AFM image. After optimizing the parameters in each step, we were able to achieve a rate of nearly 100% for capturing and releasing one gold nanoparticle, which was completed within 10 min except for the surface modification process of 30 min. The accuracy of the releasing position is estimated as nearly $2.5 \mu\text{m}$ within the light collection area. On the other hand, AFM has been widely used as a tool for the precise manipulation of individual nanoparticles including noble-metal nanoparticles with nanometer accuracy, which generally pushes or pulls nanoparticles within a single surface.^{17,18} Because the thiol-gold binding energy is $3.07 \times 10^{-19} \text{ [J/molecule]}$,¹⁹ the released particle can be pushed by the AFM tip when the number of thiol groups and the spring constant of AFM cantilever are optimized. Thus, the combination of the conventional AFM manipulation and the above technique under microscope observation is expected to be a powerful fabrication method for a plasmonic device.

In conclusion, we have demonstrated a simple method for the selection of individual plasmon-resonant nanoparticles from metal ones with various LSP characteristics on the glass substrate and its transfer to another surface under

the air environment. The recent theoretical study suggests that the LSP excitation efficiency of a single plasmon-resonant metal nanoparticle attached to dielectric microspheres can be greatly enhanced by cavity resonances in the microspheres without significant degradation of the resonators, which predicts additional SERS enhancement factors of 10^3 – 10^4 for realistic experimental conditions.²⁰ Our present technique can be used directly to fabricate this plasmonic-photonic device and this work is under way.

The present work was partly supported by funding from the Ministry of Education, Culture, Sports, Science, and Technology of Japan: KAKENHI Grant-in-Aid for Scientific Research on the Priority Area “Strong Photon-Molecule Coupling Fields” (No. 470, 1904900209) and for Young Scientists (B) (2171009009) to Y.T.

¹U. Kreibig and M. Vollmer, *Optical Properties of Metal Clusters* (Springer, Berlin, 1995).

²M. Moskovits, *Rev. Mod. Phys.* **57**, 783 (1985).

³M. Moskovits, *J. Raman Spectrosc.* **36**, 485 (2005).

⁴K. Kneipp, H. Kneipp, I. Itzkan, R. R. Dasari, and M. S. Feld, *J. Phys.: Condens. Matter* **14**, R597 (2002).

⁵T. Neumann, M.-L. Johansson, D. Kambhampati, and W. Knoll, *Adv. Funct. Mater.* **12**, 575 (2002).

⁶W. Srituravanich, N. Fang, C. Sun, Q. Luo, and X. Zhang, *Nano Lett.* **4**, 1085 (2004).

⁷A. Sundaramurthy, P. J. Schuck, N. R. Conley, D. P. Fromm, G. S. Kino, and W. E. Moerner, *Nano Lett.* **6**, 355 (2006).

⁸K. Ueno, S. Juodkazis, T. Shibuya, Y. Yokota, V. Mizeikis, K. Sasaki, and H. Misawa, *J. Am. Chem. Soc.* **130**, 6928 (2008).

⁹T. Klar, M. Perner, S. Grosse, G. von Plessen, W. Spirkl, and J. Feldmann, *Phys. Rev. Lett.* **80**, 4249 (1998).

¹⁰T. Itoh, V. Biju, M. Ishikawa, Y. Kikkawa, K. Hashimoto, A. Ikehata, and Y. Ozaki, *J. Chem. Phys.* **124**, 1347081 (2006).

¹¹S. M. Nie and S. R. Emery, *Science* **275**, 1102 (1997).

¹²H. X. Xu, E. J. Bjerneld, M. Kall, and L. Borjesson, *Phys. Rev. Lett.* **83**, 4357 (1999).

¹³E. Pavlovic, A. P. Quist, U. Gelius, and S. Oscarsson, *J. Colloid Interface Sci.* **254**, 200 (2002).

¹⁴C. M. Halliwell and A. E. G. Cass, *Anal. Chem.* **73**, 2476 (2001).

¹⁵K.-H. Su, Q.-H. Wei, X. Zhang, J. J. Mock, D. R. Smith, and S. Schultz, *Nano Lett.* **3**, 1087 (2003).

¹⁶E. Hao and G. C. Schatz, *J. Chem. Phys.* **120**, 357 (2004).

¹⁷T. Junno, K. Deppert, L. Montelius, and L. Samuelson, *Appl. Phys. Lett.* **66**, 3627 (1995).

¹⁸L. Tong, T. Zhu, and Z. Liu, *Appl. Phys. Lett.* **92**, 023109 (2008).

¹⁹P. E. Sheehan and L. J. Whitman, *Phys. Rev. Lett.* **88**, 156104 (2002).

²⁰K. A. Fuller and D. D. Smith, *Opt. Express* **15**, 3575 (2007).